The Effects of β-Aminopropionitrile on the Growing Rat Lung

Kozui Kida, MD, and W. M. Thurlbeck, MB, ChB

β-Aminopropionitrile (βAPN), 500 ng/g body weight was injected intraperitoneally into male rats every 2 days between 2 and 28 days after birth. The lungs were examined structurally and functionally and compared with the lungs of control animals given injections of saline and 28-day-old normal male rats which were not given injections. Lung volumes, both distended with air at 30 cm H_2O and with formalin at 25 cm H_2O, were increased in βAPN-treated animals. The architecture of the lung was altered so that there was a large increase in the "core," or air internal to the alveoli of the walls of alveolar ducts and sacs. Animals given injections of βAPN had 40–56% fewer alveoli than those given saline injections and normal animals. Experimental animals had larger alveoli. The lungs of βAPN-treated animals were hypercompliant, and their pressure-volume curves were shifted upward and to the left. There were morphologic changes in collagen and elastic tissue, which were more apparent in the elastic tissue. Since βAPN interferes with the synthesis of elastin and collagen, it appears that alterations in the collagen-elastin network reduces alveolar multiplication in the postnatal period. Control animals given saline had abnormal lungs when compared with normal animals. Their alveoli were larger, and they had fewer alveoli per unit volume. Thus the lung may be sensitive to relatively minor insults in the postnatal period. (Am J Pathol 1980, 101:693–710)

ALVEOLI are absent in rats and mice at birth, and most alveoli are added after birth in the human.[1] The process of alveolarization has been well studied in rats, mice, and rabbits.[1] In the first two species, the terminal gas-exchanging structures at birth have no adult counterpart; and these tubular, relatively smooth-walled, simple structures with a double capillary wall are called primary saccules. They are then subdivided by secondary crests, and the process of subdivision results in formation of alveoli and alveolar ducts and sacs. One hypothesis suggests that elastic tissue plays a key role in alveolarization,[2] since the appearance of elastic fibers precedes alveolar development and they are constantly found at the free edge of the secondary crests and at the mouths of alveoli.[3,4] This mechanism can be described simplistically. The elastin network has the appearance of a fishnet, and it is as though the lung parenchyma is an infinitely compliant balloon that is blown through a rigid fishnet, forming alveoli by protrusion through the spaces. Collagen is also involved in this scaffold, since electron-microscopic studies have shown a

From the Department of Pathology, University of British Columbia, Vancouver, British Columbia.
Supported by Grant MA-7124 from the Medical Research Council of Canada.
Accepted for publication July 1, 1980.
Address reprint requests to W. M. Thurlbeck, MB, ChB, Department of Pathology, University of British Columbia, Faculty of Medicine, 2211 Wesbrook Mall, Vancouver, British Columbia, Canada V6T 1W5.

0002-9440/80/1209-0693$01.00

constant association between collagen, elastin, and basal lamina at the margins of the crests and around the mouths of alveoli.[3] Events are less clear in the human, but elastic tissue is thought to play a similar role in postnatal alveolar multiplication.[2]

If the collagen–elastin network plays a key role in controlling alveolarization, experimental disturbance of elastogenesis and collagen formation should diminish or suppress alveolarization. To test this hypothesis, we have administered β-aminopropionitrile (βAPN) to neonatal rats and studied lung growth with particular emphasis on alveolar multiplication. βAPN interferes with cross-linking of elastin and collagen by specific inhibition of lysyl oxidase.[5]

Materials and Methods

From pilot experiments, we ascertained a dose of βAPN which, when injected intraperitoneally every 2 days during the first 4 weeks of life, appeared to produce morphologic alterations in the elastic fibers of rat lung, yet did not markedly affect somatic growth or the nutritional state of the animals. One gram of β-aminopropionitrile fumarate (Sigma Chemical Co., St. Louis, Mo) was dissolved in 10 ml sterilized physiologic saline, and 5 μl/g body weight was injected intraperitoneally with a microsyringe.

Sixteen pregnant Sprague–Dawley rats (Canadian Breeding Farm and Lab. Limited, Quebec) were randomly divided into three groups. In Group A, 7 pregnant rats produced 74 littermates, which were treated with the βAPN solution from Day 2 (the day after birth), and every second day thereafter until they were 4 weeks of age. In Group B (control), 64 littermates from 5 pregnant rats were given injections of sterilized physiologic saline (5 μl/g body weight) intraperitoneally. Twenty-seven littermates from 4 pregnant rats were used to study normal somatic and lung growth, and Group C consisted of 4-week-old rats. The animals were kept in a room with controlled temperature and supplied with standard rat chow and water *ad libitum*. Eight male rats were selected from Group A, 7 male rats from Group B, and 6 male rats from Group C for morphometric studies and pulmonary pressure–volume studies. These were from different litters in each group and represented the first animals in which successful, leak-free pressure–volume curves were obtained. Saline pressure–volume curves were attempted on other animals but were unsuccessful because of leaks in the βAPN-treated animals. The animals were sacrificed by exsanguination via the abdominal aorta under pentobarbital anesthesia. Five βAPN-treated and five saline-injected animals were used for electron-microscopic studies and were similarly sacrificed. The body weights were measured before the animals were killed. The right femur was removed, and the length from the top of the medial condyle was measured.

Pressure-Volume Measurements

Following anesthesia and exsanguination of the animals, a midsternotomy incision was made. An endotracheal tube (22 G of Medicut Cannula, Sherwood Medical Industries, St. Louis, Mo) was inserted, and the heart and lungs were removed *en bloc*. After a brief rinse in physiologic saline, the lungs were placed in a vacuum jar and degassed to a pressure of 200 mm Hg. The endotracheal tube was connected by a Y-connector to a syringe that was attached to one limb and a Statham p-23BB pressure transducer (Statham Instruments, Inc., Hato Ray, Puerto Rico) connected to the other limb. Pressures were read from a galvanometer (Model 310, Triplett Co.), calibrated by a water manometer. Lungs were inflated with air to a transpulmonary pressure of 30 cm H_2O. The air volume at this point

was designated as V_{30}. The lungs appeared completely inflated at this point. Portions of air, 0.1 ml, were then withdrawn from the lung, and the pressures at each point were measured. Pressures were recorded after the needle of the galvanometer had been stabilized for at least 15 seconds at each pressure point. The second deflation limb was recorded for pressure–volume studies. If the pressure did not remain constant, this was regarded as evidence of an air leak and the lungs were discarded. Correction was made for the Boyle's law effect. All the measurements were performed within 30 minutes after death. The data were analyzed by fitting an exponential to the pressure–volume curve with the use of a digital computer according to the methods of Colebatch and associates [6] and differed in that all the data points greater than or equal to 40% of V_{30} were included in the data calculations. An iterative least mean squares technique was used to solve the equation $V = V_{max} - Be^{-KP}$ where V is the volume at pressure P, V_{max} the theoretical volume at infinite pressure, and B is the difference between V_{max} and the intercept of the fitted exponential on the volume axis. The continuous change in the slope of the PV curve is quantitated by K in units cm H_2O^{-1}. B/V_{max} ratio quantitates the position of the curve. Static compliance, expressed as air volume (ml) per cm H_2O and as a percentage of maximum lung volume as determined from the exponential fit per cm H_2O was obtained from a slope of the regression line whose data points were between 40% and 70% of maximum lung volume.

After completion of the pressure–volume measurements, the lungs were separated from the heart and the thymus, weighed, and then inflated at a constant pressure of 25 cm of formalin for at least 72 hours. Fixed lung volume (V_L) was measured by water displacement at the end of the period of fixation. A block of tissue was obtained from the left lung by sectioning longitudinally along the bronchus. Paraffin-embedded tissue blocks were cut into 5-μ thicknesses, and the first section beyond the bronchus was used for morphometry with modifications [7] of standard morphometric techniques. Shrinkage during tissue processing was measured. In addition, sections were stained with Humberston's elastic fiber stain. The following measurements and calculations were made on hematoxylin-and-eosin–stained section: Mean interalveolar wall distance (Lm; μ), alveolar surface area (sq m), number of alveoli per unit area (sq cm) and volume (ml), total number of alveoli per lung, average alveolar volume (cu μ), surface-to-volume ratio of alveoli (cm^{-1}), and the volume proportions of alveolar air, alveolar duct air, bronchial and bronchiolar air (conducting airway air), alveolar wall tissue, blood vessels and lymphatics, bronchial and bronchiolar wall tissue (conducting airway wall), and connective tissue. Alveolar duct air was defined as a "core" of air lying internal to the mouths of alveoli in alveolar sacs and ducts. Absolute measurements were corrected for tissue shrinkage during processing and refer to V_{30}. It was assumed that dimensions of structures and volume proportions were the same in the right (unmeasured) lung as in the left (measured) lung.

For transmission electron microscopy, the lungs were fixed with a solution of 2.5% glutaraldehyde in 0.05 M cacodylate buffer (pH 7.4) for 1 hour at 4 C. After a brief washing in 0.05 M cacodylate buffer, the tissue was postfixed in 1% osmium tetroxide and 0.05 M cacodylate buffer, *en bloc* stained with an 0.2% uranyl acetate solution for 30 minutes, and embedded in Epon 812. Standard procedures were followed. Semithin (1-μ) sections were stained with Richardson's stain for light-microscopic examination. Ultrathin sections were stained in uranyl acetate and lead citrate and observed with a Philips EM300 electron microscope (60kV). Ruthenium red staining was applied to some of the blocks according to the method of Luft. [8] For scanning electron microscopy, the opposite lungs were fixed with the use of an intratracheal glutaraldehyde solution at a constant pressure of 25 cm H_2O for 1 hour and postfixed in buffered osmium tetroxide. The dehydrated tissue blocks were put into a freeze dryer (Unitrap II, Vertis Co., Gardiner, New York) overnight and coated with gold. Observations were made with the use of a Super-SEM ISI (25 kV) (International Scientific Instruments, Palo Alto, Calif).

Statistical evaluation of the data was performed with the use of the Student *t* test for grouped data. Probabilities of less than 0.05 were considered significant.

Results

Table 1 shows that no significant differences in body size and lung weight were apparent between the control animals given saline injections (Group B) and the normal animals (Group C). Lung volumes were greater in the βAPN-treated animals.

The gross appearance of the lungs was similar in all the animals, and the pleural surfaces appeared smooth in all. Often there were obvious microscopic abnormalities on subjective assessment of the sections of the βAPN-treated animals, which showed a striking enlargement of both the alveoli and alveolar ducts, without alveolar wall rupture (Figure 1). The changes in architecture were distributed throughout the entire lung, and no obvious differences were observed in air space size between the surface (close to the pleura) and the deeper areas. Stains for elastic tissue showed that the elastic fibers appeared equally reduced throughout the alveolar wall, including the mouths of the alveoli, the airways, the blood vessels, and the pleura.

Scanning Electron Microscopy

Photomicrographs (Figure 2) from both the βAPN-treated lung and the control lung emphasized the changes seen by light microscopy. Alveoli were larger, and alveolar duct air was increased. No increase in pores of Kohn or fenestrae of alveolar walls was observed.

Transmission Electron Microscopy

Special attention was given to the study of ultrastructural changes in extracellular components. The ultrastructure of the subpleural region was studied for two reasons. First, it is an easily identified region of the lung, and it therefore easy for one to compare similar areas of different animals. Second, the distribution and structure of elastic fibers were similar to other regions of the lung that are less clearly identified.

In the control lungs, the elastic lamina of the pleura appeared as continuous thick bands (Figure 3A), whereas that in the βAPN-treated lung was thinner, more irregular, and apparently focally fragmented (Figure 3B). Elastic fibers were formed from amorphous material (elastin) and a number of microfibrils, which surrounded the elastin as seen in normal elastic fibers. Tannic acid staining, which stains elastin, showed that, although the ultrastructure of the elastic fibers of βAPN-treated animals was different from that of the normal lungs in terms of size, the central amorphous material stained the same in both groups. In places, the alveolar epithelial basal lamina appeared thicker than normal, but these changes were focal and inconstant. The acid mucopolysaccharides in the

Table 1—Body Weight, Femur Length, and Lung Size (Mean ± SE)

Group	Body weight (g)	Femur length (mm)	Fresh lung weight (g)	V_{30} (ml)	Fixed lung volume (ml)	Specific lung volume (ml/100 g body weight)
A: βAPN-treated (n = 8)	76.38 ± 3.36	21.3 ± 0.5	1.06 ± 0.04	5.60 ± 0.36	6.54 ± 0.31	8.645 ± 0.464
B: Saline-treated (n = 27)	78.68 ± 3.92	21.1 ± 0.5	0.94 ± 0.06	4.66 ± 0.10	4.81 ± 0.35	6.243 ± 0.535
C: Not treated (n = 6)	77.67 ± 3.92	21.0 ± 0.3	1.01 ± 0.06	4.62 ± 0.15	4.88 ± 0.26	6.356 ± 0.450
P value						
A vs B	NS	NS	NS	$0.02 < P < 0.05$	$0.001 < P < 0.01$	$0.001 < P < 0.01$
A vs C	NS	NS	NS	$0.02 < P < 0.05$	$0.001 < P < 0.01$	$0.001 < P < 0.01$
B vs C	NS	NS	NS	NS	NS	NS

extracellular matrix, which are identified by *en bloc* ruthenium red staining, showed no remarkable changes. The collagen fibers in the βAPN-treated lung were loosely arranged, and their diameters in cross-section varied widely (Figure 4A), as compared with the control lungs (Figure 4B). However, the characteristic periodicity of the collagen fibers in both βAPN-treated and control lungs did not show any detectable difference.

Morphometry

The morphometric results are shown in Table 2. The interalveolar wall distance of the βAPN-treated animals was about 25% larger (140.73 μ) than those of Groups B and C, with 112.66 μ and 105.44 μ, respectively. The internal geometry of the lung was significantly altered, with a marked increase in alveolar duct air proportion in the βAPN-treated animals (0.389), compared with the saline-treated control animals (0.233) or the normal animals (0.222). Since the lung volumes were greater in the βAPN-treated animals, this represented a considerable increase in the volume of air in their alveolar ducts. In contrast, alveolar proportion was reduced in the βAPN-treated animals (0.405), compared with the saline-treated (0.566) or normal animals (0.580). The increase in lung volume in the βAPN-treated animals was not sufficiently great to compensate for the decrease in alveolar air proportion in the βAPN-treated animals, so that the volume of air in the alveoli was decreased (2.494 ml), compared with the saline-heated (3.280 ml) or normal animals (3.241 ml). Since there were substantially fewer alveoli in the βAPN-treated animals, average alveolar volume was increased in the βAPN-treated animals (27.116×10^4 cu μ) compared to the saline-injected (22.39×10^4 cu μ) or normal animals (17.438×10^4 cu μ). Thus the morphometric results confirmed the subjective assessment of the changes, with a great increase in the core of air internal to alveoli in alveolar ducts and sacs and a modest increase in size of alveoli. βAPN-treated animals had about half the number of alveoli per unit volume of lung, and the total number of alveoli was markedly reduced, compared with saline-treated and normal rats, the βAPN-treated animals having 10 million alveoli in their lungs, compared with 20 million in the control animals and 25 million in the normal animals. Alveolar surface area was significantly diminished in the βAPN-treated animals, compared with the normal animals, despite an increase in lung volume reflecting a simplification of the gas-exchanging area in the βAPN-treated animals. Further confirmation of this is given by the surface-to-volume ratio, which is decreased in the βAPN-treated animals. No significant alterations were found in the volume proportions or absolute volumes of alveolar wall, conducting air, blood vessel, conducting air-

Table 2—Morphometric Data

Group	Volume proportion (mean ± SE)						
	Alveolar air	Duct air	Alveolar wall	Conducting air	Blood vessels	Conducting wall	Connective tissue
A: βAPN-treated (n = 8)	0.405 ± 0.030	0.389 ± 0.033	0.133 ± 0.005	0.019 ± 0.007	0.027 ± 0.008	0.004 ± 0.001	0.024 ± 0.010
B: Saline-treated (n = 7)	0.566 ± 0.022	0.233 ± 0.023	0.125 ± 0.004	0.039 ± 0.011	0.022 ± 0.005	0.007 ± 0.002	0.009 ± 0.003
C: Not treated (n = 6)	0.580 ± 0.009	0.222 ± 0.016	0.139 ± 0.010	0.018 ± 0.008	0.026 ± 0.006	0.007 ± 0.003	0.009 ± 0.004
P value							
A vs B	$P < 0.001$	$0.001 < P < 0.01$	NS	NS	NS	NS	NS
A vs C	$P < 0.001$	$0.001 < P < 0.01$	NS	NS	NS	NS	NS
B vs C	NS	NS	NS	NS	NS	NS	NS

Table 2—(continued)

Group	Mean interalveolar wall distance: Lm (μ)	Volume proportion duct air × Lm (μ)	Alveolar surface area (sq m)	$N_A \times 10^{-4}$	$N_v \times 10^{-5}$	NAT $\times 10^{-6}$	Average alveolar volume $\times 10^{-4}$ (cu μ)	$S_v \times 10$ (cm^{-1})
A: βAPN-treated: (n = 8)	140.73 ± 4.43	54.79 ± 5.02	0.1755 ± 0.0119	1.365 ± 0.096	16.561 ± 1.670	10.268 ± 1.407	27.116 ± 1.757	2.863 ± 0.093
B: Saline-treated (n = 7)	112.66 ± 4.05	26.19 ± 2.73	0.2086 ± 0.0128	2.532 ± 0.079	34.687 ± 1.640	20.077 ± 1.072	22.039 ± 0.482	3.580 ± 0.138
C: Not treated (n = 6)	105.44 ± 2.35	23.32 ± 1.48	0.2125 ± 0.0115	3.004 ± 0.126	44.214 ± 2.773	24.748 ± 2.044	17.438 ± 1.086	3.803 ± 0.083
P value								
A vs B	$P < 0.001$	$P < 0.001$	NS	$P < 0.001$	$P < 0.001$	$P < 0.001$	$0.02 < P < 0.05$	$P < 0.001$
A vs C	$P < 0.001$	$P < 0.001$	$0.02 < P < 0.05$	$P < 0.001$	$P < 0.001$	$P < 0.001$	$0.001 < P < 0.01$	$P < 0.001$
B vs C	NS	NS	NS	$0.001 < P < 0.01$	$0.01 < P < 0.02$	NS	$0.001 < P < 0.01$	NS

N_A = number of alveoli/sq cm; N_v = number of alveoli/ml; NAT = total number of alveoli; S_v = surface-to-volume ratio.

way wall, or connective tissue. Saline-treated animals generally had values between the βAPN-treated animals and the normal animals, but the differences between normal and saline-treated animals was only statistically significant for number of alveoli per unit area and volume and for average alveolar volume.

Pressure–Volume Curves

The pressure-volume curves showed abnormalities in the βAPN-treated animals, and the pressure–volume curves of the saline-treated animals and the normal animals were indistinguishable from each other. This is true whether the pressure–volume curves are expressed as absolute lung volumes (Text-figure 1) or as a percentage of maximum lung volume (V_{max}) predicted from an exponential fit (Text-figure 2). These changes are greater when expressed as absolute lung volumes, and the differences are significant in the βAPN-treated animals at all transpulmonary pressure equal to or greater than 5 cm H_2O. When expressed as a percentage of V_{max}, the differences are significant at all transpulmonary pressures of 10 cm H_2O or greater. Expression of the pressure–volume curves shows that

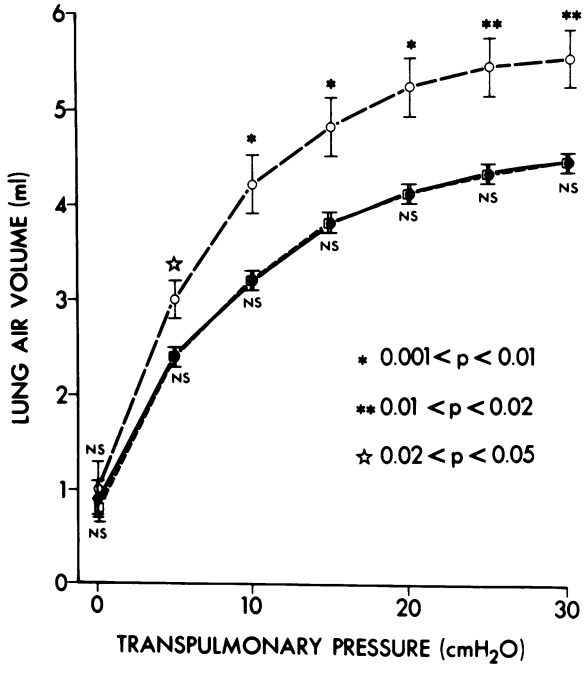

TEXT FIGURE 1—Air-filled pressure–volume curves mean ±SE). Actual lung volume (ml) against transpulmonary pressure (cm H_2O). — — O — — –, βAPN-treated group; – – – □ – – –, non-treated group; ——●——, saline-treated group.

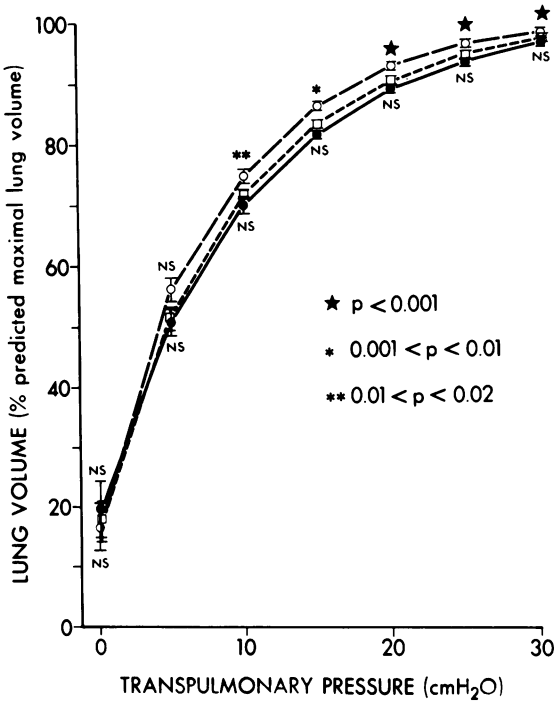

TEXT-FIGURE 2—Air-filled pressure–volume curves (mean ± SE). Percent of maximum lung volume at infinite pressure against transpulmonary pressure. ——O——, βAPN-treated group; - - -□- - -, non-treated group, ——●——, saline-treated group.

(Table 3) the shape constant (K) is significantly increased, V_{max} is significantly increased, and compliance is also significantly greater in βAPN-treated animals, compared with saline-treated and normal animals, whether expressed in absolute lung volumes or as a percentage of V_{max}.

Discussion

The objective of the present study was to evaluate the role that elastic fibers and/or collagen fibers play in the growing lung. The data show that βAPN interferes with normal connective tissue formation as assessed subjectively by light- and electron-microscopic examination, resulting in enlarged alveolar ducts and modestly enlarged alveoli that are diminished in number as compared with control and normal animals. In addition, there are associated abnormalities of the pressure–volume curve, with large lung volumes in the βAPN-treated animals, together with increased compliance and a shift of the pressure–volume curve upward and to the left.

We do not have biochemical proof of alterations in elastin and/or collagen in our animals, nor can we ascribe with certainty the changes in the

Table 3—Pressure–Volume Measurements (Mean ± SE)

	K	V_{max}	b	Compliance I	Compliance II	Exponential equation
A: βAPN-treated (n = 8)	0.125 ± 0.005	5.585 ± 0.341	4.751 ± 0.288	0.303 ± 0.024	5.438 ± 0.353	$V = 5.585 - 4.751e^{-0.225p}$
B: Saline-treated (n = 7)	0.099 ± 0.003	4.649 ± 0.105	3.733 ± 0.253	0.184 ± 0.013	3.948 ± 0.263	$V = 4.649 - 3.733e^{-0.099p}$
C: Not treated (n = 6)	0.107 ± 0.004	4.553 ± 0.153	3.733 ± 0.105	0.187 ± 0.020	4.065 ± 0.317	$V = 4.553 - 3.733e^{-0.107p}$
P value						
A vs B	$P < 0.001$	$0.02 < P < 0.05$	$0.02 < P < 0.05$	$0.001 < P < 0.01$	$0.001 < P < 0.01$	
A vs C	$0.02 < P < 0.05$	$0.02 < P < 0.05$	$0.01 < P < 0.02$	$0.001 < P < 0.01$	$0.001 < P < 0.02$	
B vs C	NS	NS	NS	NS	NS	

K, V_{max}, and b are constants in a single exponential, which is expressed as $V = V_{max} - be^{-Kp}$, where V_{max} is the volume at ∞ pressure, and V the lung volume at pressure p.

Compliance I: compliance expressed as volume (ml)/(cm H_2O), at 40–70% V_{max}.

Compliance II: compliance expressed as % V_{max}/(cm H_2O), at 40–70% V_{max}.

pressure–volume curves to alteration in tissue forces, since we were unable to perform satisfactory saline-filled pressure–volume curves in the βAPN animals because of leaks into the interstitium. There is, however, good evidence that βAPN alters collagen and elastin by preventing cross-linking in these tissues in several organs,[9] but the effect on the lungs is less well documented. Incomplete cross-linking, as assessed by aldehyde content, have been described in rats following βAPN administration and was accompanied by marked changes in lung compliance in young rats and small changes in older rats.[10] Minimal changes are to be anticipated, since most connective tissue is laid down early in postnatal life [11] and the turnover of collagen and elastin in the lung is slow.[12] Under these circumstances βAPN does not affect preformed collagen and elastic tissue, and one would anticipate minimal biochemical, physiologic, and anatomic effects in older animals. Indeed, no anatomic changes were found when βAPN was administered to mature hamsters.[13] Several authors [14–17] have successfully performed both saline- and air-filled pressure–volume curves in animals whose connective tissue was affected by elastase or collagenase and in blotchy mice. These authors found that the changes were due to alterations in tissue, rather than surface, forces. Another lathyrogen, semicarbazide, has been show to alter saline pressure–volume curves.[18] Alterations in air-filled pressure-volume curves have been noted in elastase-treated lungs [16] and in animals given D-penicillamine,[19] another lathyrogen, and were considered to be due to changes in tissue forces. We thus feel that it is likely that the alterations in the pressure–volume curve in our animals are due to changes in tissue forces, because of the visually observed alterations in elastin and collagen, the evident fragility of the lungs, and the published work of others.

Most other experiments designed to affect the connective tissue framework of the lung differ in that weanling or older animals have been used. By this time most of the connective tissue of the lung has been laid down and alveolar formation is far advanced. Two experiments are of direct relevance. Fisk and Kuhn [17] studied the lungs of blotchy mice that have a congenitally acquired defect so that the lysine-derived aldehydes necessary for cross-linking of elastin and collagen cannot be generated. O'Dell et al [20] produced copper deficiency in suckling rats. Copper deficiency reduces lysyl oxidase activity and hence diminished cross-linking of collagen and elastin. In both experiments, the animals had lungs that were disproportionately large and morphologically abnormal. Although the morphometric data are not complete in either study, evidence is presented in both that the lungs have lower surface-to-volume ratios, suggesting simplification of lung structure with too few or too large alveoli. Fisk and

Kuhn [17] and O'Dell et al [20] concluded that they had produced emphysema, whereas we have concluded that alveolar multiplication has been hindered. The issue may not be important. Elsewhere, one of us [21] has pointed out the resemblance between the neonatal lung and advanced elastase-induced emphysema as well as the reciprocal morphologic appearance of advancing alveolarization in the developing lung and the progressive loss of alveoli in elastase-induced emphysema. This was used as an argument for the importance of elastic tissue in formation of alveoli in the neonatal period and for the significance of destruction of elastic tissue in the pathogenesis of emphysema.

Although lathyrogens affect both collagen and elastin cross-linking, it appears that some may affect one protein more than another. Semicarbazide appeared to affect collagen more than elastin in rat lung,[18] and D-penicillamine affected elastin more than collagen in hamster lung.[19] Striking changes were seen electron-microscopically in elastin in copper-deficient rats, whereas changes in collagen were not apparent.[20] In our experiments, both collagen and elastin appeared to be affected ultrastructurally, but perhaps elastin was affected more. The pressure–volume data, with alteration of compliance in the mid-lung volume range, suggests that the elastic tissue was affected. At first sight, the large increase in V_{30} might suggest that collagen was affected, since the Setnikar-Mead model [22] of lung distensibility predicts that at high lung volume the stretched collagen provides the recoil force and limits lung distensibility. However, it is well-recognized that increased lung volumes are characteristic of elastase-induced emphysema.[15] Karlinsky and his colleagues [15] have studied this apparent anomaly and have shown that while *in vivo* administration of elastase produced increased lung volumes, *in vitro* incubation of lung with elastase did not have this result. They have suggested a number of possibilities for this difference, such as elaboration of collagenase by the inflammatory exudate resulting from administration of elastase, unhooking of elastic tissue–collagen attachments that might only occur in the *in vivo* model, or a possible glue-like function of proteoglycans producing a functional association of collagen and elastin that only disturbed in the *in vivo* model. Biochemical studies of our experimental protocol might provide useful information about this interesting problem, and we hope that other investigators will address themselves to it.

It should be noted that saline injection alone generally altered the morphometric variables toward those of the βAPN-treated animals. As pointed out, only the number of alveoli per unit volume and area and average alveolar volume were significantly altered, but it appears that saline injection alone *per se* may alter lung growth. This suggests that minimal

insults in early life may affect lung growth. If this is the case, then there may be important implications. Older patients with chronic air flow limitation have a history of more frequent respiratory illnesses in childhood.[23] Perhaps these insults interfered with lung growth and predisposed the lung to injury by cigarette smoke in adult life. This is one possible explanation for the widely differing response of the lung to injury.

References

1. Thurlbeck WM, Wang NS: Structure of the lung, Respiratory Physiology. Edited by JG Widdicombe. Series edited by C. Guyton. Baltimore, University Park Press, 1970, pp 1–30
2. Emery JL: The postnatal development of the human lung and its implications for lung pathology. Respiration 1970, 27 (Suppl):41–50
3. Amy RWM, Bowes D, Burri PH, Haines J, Thurlbeck WM: Postnatal growth of the mouse lung. J Anat 1977, 124:131–151
4. Loosli CG, Potter EL: Pre- and postnatal development of the respiratory portion of the human lung with special reference to the elastic fibers. Am Rev Respir Dis 1959, 80(Part 2): 5–23
5. Page RC, Benditt EP: Molecular diseases of connective and vascular tissues: II. Amine oxidase inhibition by the lathyrogen, β-aminopropionitrile. Biochemistry 1967, 6:1142–1148
6. Colebatch HJH, Ng, CKY, Nikov N: Use of an exponential function for elastic recoil. J Appl Physiol 1979, 46:387–393
7. Holmes C, Thurlbeck WM: Normal lung growth and response after pneumonectomy in rats at various ages. Am Rev Respir Dis 1979, 120:1125–1136
8. Luft JH: Fine structure of capillary and endocapillary layer as revealed by ruthenium red. Fed Proc 1966, 25:1773–1783
9. Siegel RC: Lysyl oxidase. Int Rev Conn Tiss Res 1979, 8:73–118
10. Goldstein ER, Haddad R, Hamosh P: Effect of β-aminopropionitrile (βAPN) on the elastic behavior of the rat lung (Abstr). Clin Res 1970, 18:89A
11. Bradley KH, McConnell SD, Crystal RG: Lung collagen composition and synthesis: Characterization and changes with age. J Biol Chem 1974, 249:2674–2683
12. Hance, AJ, Crystal RG: Collagen, The Biochemical Basis of Pulmonary Function. Edited by RG Crystal. Series: Lung Biology in Health and Disease. Vol 2. New York, Marcel Dekker, 1976, pp 215–271
13. Kuhn C, Starcher B: The significance of connective tissue repair in elastase-induced emphysema (Abstr). Am Rev Respir Dis 1976, 113 (Suppl):209
14. Koo KW, Hayes JA, Kagan HM, Leith DE, Franzblau C, Snider GL: Lung volumes and mechanics following elastase and collagenase in hamsters (Abstr). Clin Res 1974, 22:508A
15. Karlinsky JB, Snider GL, Franzblau C, Stone PJ, Hoppin FG Jr: *In vitro* effects of elastase and collagenase on mechanical properties of hamster lungs. Am Rev Respir Dis 1976, 113:769–777
16. Johanson WG Jr, Pierce AK: Effect of elastase, collagenase, and papain on structure and function of rat lung in vitro. J Clin Invest 1972, 51:288–293
17. Fisk DE, Kuhn C: Emphysema-like changes in the lungs of the blotchy mouse. Am Rev Respir Dis 1976, 113:787–797
18. Stanley NN, Alper R, Cunningham EL, Cherniack NS, Kefalides NA: Effects of a molecular change in collagen on lung structure and mechanical function. J Clin Invest 1975, 55:1195–1201

19. Hoffman L, Mondshine RB, Park SS: Effect of DL-penicillamine on elastic properties of rat lung. J Appl Physiol 1971, 30:508–511
20. O'Dell BL, Kilburn KH, McKenzie WN, Thurston RJ: The lung of the copper-deficient rat: A model for developmental pulmonary emphysema. Am J Pathol 1978, 91:413–432
21. Thurlbeck WM: Aspects of chronic airflow obstruction. Chest 1977, 72:341–330
23. Burrows B, Knudson RJ, Liebowitz MD: The relationship of childhood illness to adult obstructive airway disease. Am Rev Respir Dis 1977, 115:751–760

Acknowledgments

We thank Mrs. Joan Mathers for carrying out the preparation of electron-microscopic studies and Mr. Wayne Galaugher for his technical advice.

[Illustrations follow]

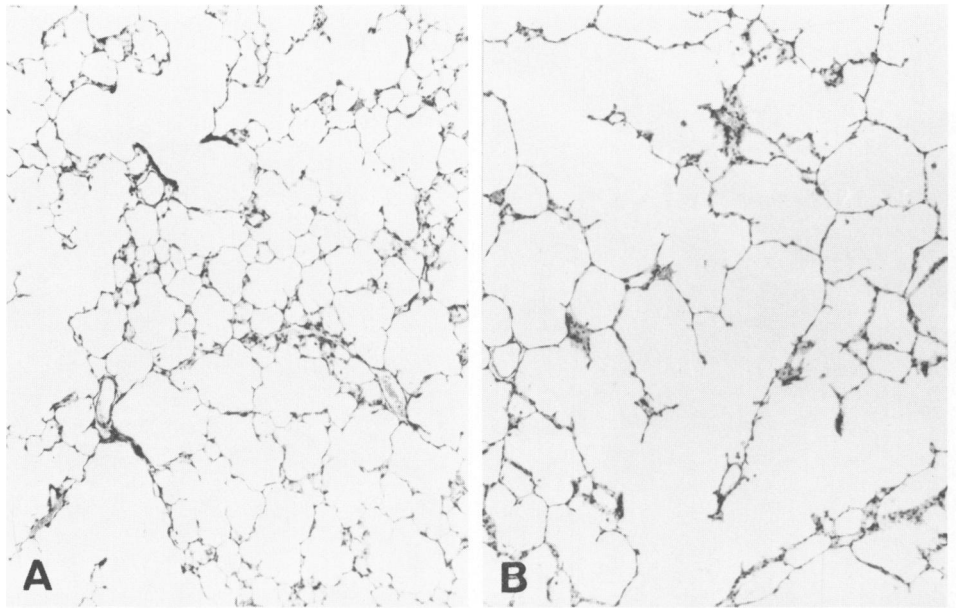

1

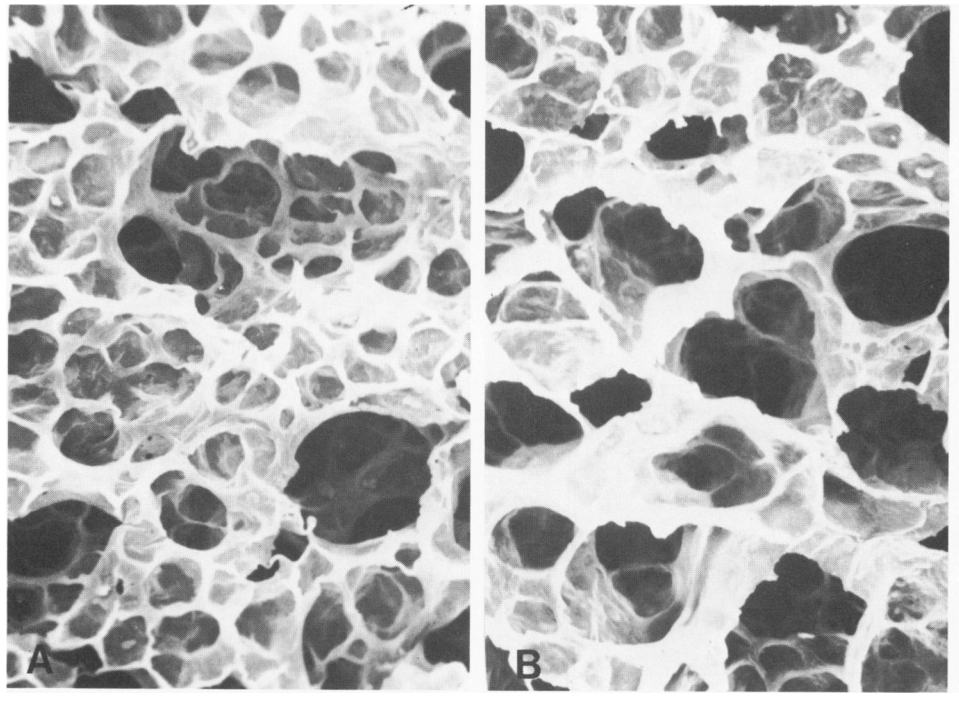

2

Figure 1 A—Lung from saline-treated (control) rat. **B**—βAPN-treated lung. Air spaces which include alveoli and alveolar ducts are markedly enlarged, but no rupture of the walls can be seen. (H&E, ×100) **Figure 2**—Scanning electron micrographs of a lung from a saline injected animal (**A**) contrasts with a βAPN-treated rat (**B**). The air spaces are enlarged and the alveoli flattened in the βAPN-treated lung. (×200)

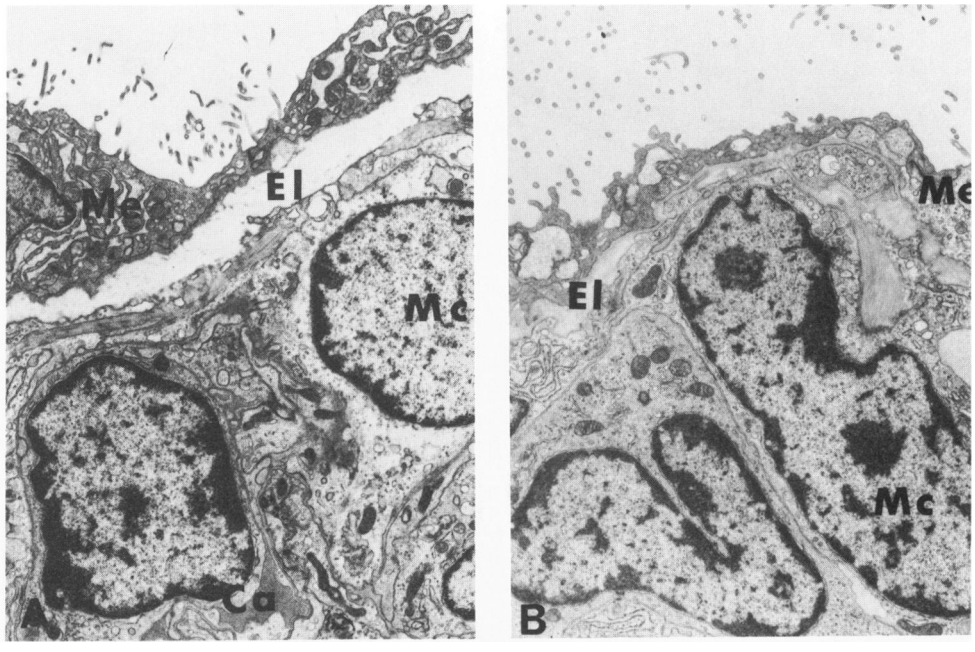

3

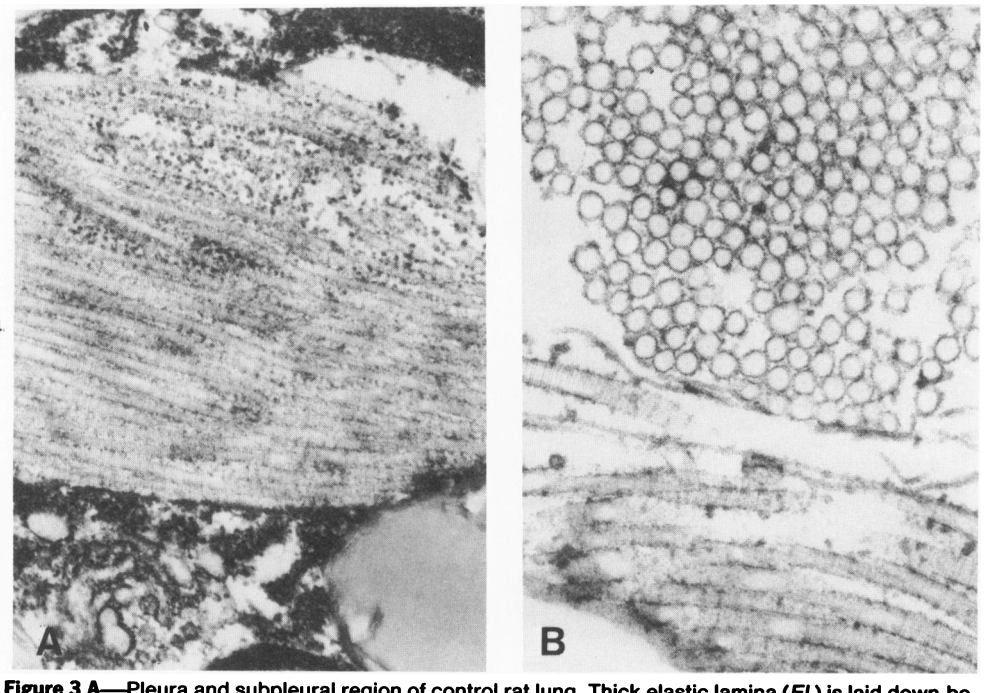

4

Figure 3 **A**—Pleura and subpleural region of control rat lung. Thick elastic lamina (*El*) is laid down beneath mesothelial cells (*Me*). A small capillary (*Ca*) and a mesenchymal cell (*Mc*) with lipid granules are seen. **B**—Pleura and subpleural region of βAPN-treated rat lung. The elastic lamina is fragmented and thin compared to the control lung. (Lead citrate and uranyl acetate, ×6000) **Figure 4** **A**—Saline-treated rat lung. The collagen fibers have a uniform diameter, compared with those of βAPN-treated lung. (Ruthenium red and lead citrate, ×30,000) **B**—βAPN-treated rat lung. The collagen fibers are loosely arranged with a wide range of diameters. Individual fibers are covered by ruthenium-red–positive materials.